Identification of electron field-aligned current systems in Saturn's magnetosphere

P. Schippers,[1,2] N. André,[3,4] D. A. Gurnett,[1] G. R. Lewis,[5,6] A. M. Persoon,[1] and A. J. Coates[5,6]

Received 9 November 2011; revised 16 March 2012; accepted 16 March 2012; published 2 May 2012.

[1] Based on the analysis of 7 years of Cassini electron plasma spectrometer data near Saturn's equatorial plane, we computed the average directional electron current in the Northern and the Southern hemispheres separately. We determined the net current density by subtracting the downward electron current density (equator to the ionosphere) from the upward electron current density (ionosphere to the equator). From the symmetric analysis (no separation in local time), we identified: (1) layers of net upward current carried by the thermal electrons (1–10 eV) in both hemispheres inside 5–8 R_S (Saturn Radius = 60,268 km) (region A) and (2) layers of net downward current carried by a population of warmer electrons (10–400 eV) inside 8–10 R_S (region B). From the analysis of the currents organized by local time (dayside and nightside parsing), new features were identified such as (1) a day-night asymmetry of the current carried by the warm and hot (400 eV–26,000 eV) electrons beyond 10 R_S (region C), and (2) the possible existence of inter-hemispheric currents directed from the Southern to the Northern hemisphere inside 4 R_S (region A) and oppositely directed at about 13–15 R_S (region C). Our interpretation is that the observed current system results from the superimposition of (1) a current system associated with the corotation enforcement, (2) a current system linked to the presence of the newly identified noon-to-midnight convection electric field and (3) a system of inter-hemispheric currents driven by the thermosphere-ionosphere. We finally discuss the relation of the observed currents with the newly identified Saturn's secondary auroral emissions.

Citation: Schippers, P., N. André, D. A. Gurnett, G. R. Lewis, A. M. Persoon, and A. J. Coates (2012), Identification of electron field-aligned current systems in Saturn's magnetosphere, *J. Geophys. Res.*, *117*, A05204, doi:10.1029/2011JA017352.

1. Introduction

[2] In planetary magnetospheres, field-aligned currents are associated with the transfer of momentum between the magnetosphere and the ionosphere. The formation of field-aligned currents may arise for different reasons: the presence of a magnetospheric convective electric field, the corotation lag of the magnetospheric plasma with respect to the neutral atmosphere, the closure of partial azimuthal equatorial currents, the precipitation of particles triggered by magnetospheric compression and transport, the presence of ionospheric winds or different conductivities in the Northern and Southern hemispheres.

[3] Some of these currents are indeed susceptible to be triggered in Saturn's magnetosphere. First, the magnetospheres of outer planets are characterized by a fast rotation implying the generation of an important corotation electric field which will drag the magnetospheric plasma in a circular motion at the planet's rotation rate. However, pick-up and transport processes will introduce a corotation lag of the plasma flow which will give rise to a transverse electric field in the ionosphere which is then transferred to the magnetosphere through field-aligned currents [*Cowley and Bunce*, 2003]. This will force the magnetospheric plasma to corotate and generate a perturbation in the azimuthal magnetic field component which can then be used as a tracer for the presence of such currents. Evidence of corotation lag has indeed been reported by *Richardson* [1998], *Saur et al.* [2004], *Wilson et al.* [2008], and *Thomsen et al.* [2010].

[4] Second, the evidence of the existence of a weak convective electric field fixed in local time (Noon to Midnight) in the inner magnetosphere was predicted by *Roussos et al.* [2007] which reported an asymmetry of the satellite absorption micro-signatures. This was then confirmed by *Paranicas et al.* [2010] which reported a dayside-nightside asymmetry of the Mev electrons in the Saturn inner radiation belt region. This dayside-nightside asymmetry is ubiquitous and observed in several other magnetospheric parameters

[1]Department of Physics and Astronomy, University of Iowa, Iowa City, Iowa, USA.
[2]Now at LESIA, Observatoire de Paris, CNRS, Meudon, France.
[3]Université de Toulouse, UPS, IRAP, Toulouse, France.
[4]CNRS, IRAP, UMR5277, Toulouse, France.
[5]Mullard Space Science Laboratory, University College London, Holmbury St. Mary, UK.
[6]The Centre for Planetary Sciences at UCL/Birkbeck, London, UK.

Corresponding Author: P. Schippers, LESIA, Observatoire de Paris, CNRS, 5 pl. Jules Janssen, F-92190 Meudon, France. (patricia.schippers@obspm.fr)

0148-0227/12/2011JA017352

such as in the ring current [*Krimigis et al.*, 2007; *Sergis et al.*, 2009] or the asymmetry of the electron flux [*DeJong et al.*, 2011]. The existence of such a local time asymmetric electric field induces the presence of an associated field-aligned current system coupling the magnetosphere to the ionosphere.

[5] Third, the Saturn's spin axis is highly inclined with respect to the ecliptic plane ($\pm 27^\circ$) which implies important seasonal effects. The Northern and the Southern hemispheres are unequally illuminated (except during Equinox periods) inducing asymmetric ionospheric conductances in both hemispheres, as illustrated by the dual character of the Saturn Kilometric Radiation and its reversal around Equinox [*Gurnett et al.*, 2010]. Under these conditions, inter-hemispheric field-aligned currents (IHFACs) may arise in the closed magnetic field lines region. *Southwood and Kivelson* [2007] inferred the existence of such IHFACs as the source of the rotating magnetic field in the inner magnetosphere identified by *Espinosa and Dougherty* [2001].

[6] The first observational evidence of field-aligned currents at Saturn was reported by *Bunce et al.* [2008] during the high-latitude phase of the Cassini mission. Based on the analysis of magnetic field perturbations, *Talboys et al.* [2009a, 2009b] identified successive layers of downward and upward current in the outer and high-latitude magnetospheric region, close to the open-closed magnetic field line boundary. *Talboys et al.* [2009a] reported that the upward current layer is co-located with the statistical location of Saturn's main auroral oval in the dayside [*Badman et al.*, 2006].

[7] In this paper, we analyze the structure of the magnetic field-aligned electron flow in the magnetosphere up to 20 R_S, near the equatorial plane. We tentatively identify the current systems, their topology, spatial asymmetry, origin and discuss their relation to the auroral signatures.

2. Dataset and Methodology

[8] We used the electron data acquired by the Electron Spectrometer (ELS) of the Cassini Plasma Spectrometer (CAPS) instrument [*Young et al.*, 2005] onboard Cassini. ELS is an electrostatic analyzer composed of 8 anodes of $5^\circ \times 20^\circ$ measuring electrons in 63 energy channels, logarithmically spaced from 0.6 eV to 26 keV. The instrument is mounted on a rotating turntable allowing an azimuthal coverage of $\pm 104^\circ$ around the spacecraft Z-axis.

[9] We selected the time periods when Cassini was near the equatorial rotational plane at a latitude between -5° and $+5^\circ$, from July 2004 to June 2011. We first binned the high resolution electron data into 10 degree wide pitch angle sectors determined by using the magnetic field data direction measured in-situ by the magnetometer MAG. We then averaged all the data at 15 min, a time resolution which allows both reasonable radial distance resolution and computing time to run a statistical analysis over a very large dataset. Then, we separated the data into Northern and Southern hemispheres using both the geographic latitude criterion and the sign of the radial component of the magnetic field B_r which can be used as an indication of the location of the plasma sheet [*Arridge et al.*, 2008] (i.e. the Northern hemisphere being defined by positive latitude and positive B_r). The location of the plasma sheet is indeed observed to be very variable in time and in local time, and these effects are observed in the magnetotail as well as in regions close to the planet [*Krimigis et al.*, 2007; *Arridge et al.*, 2008; *Carbary et al.*, 2008; *Khurana et al.*, 2009]. After parsing the dataset into Northern and Southern hemispheres, we binned each dataset in radial distance, into 0.2 R_S wide intervals from 3 to 20 R_S. We considered two cases: 1) the 'symmetric' case, where we merged all the data and assumed no longitude and no local time dependence, and 2) the local time (LT) dependent case, where we separated the whole dataset into dayside (from 0700 to 1700 LT) and nightside (from 1900 to 0500 LT) local times. We finally determined the median of the energy flux and its uncertainty in each energy bin and direction. We calculated the net field-aligned current density $j = qN_e v$ (where q is the electric charge, N_e the electron number density and v the electron velocity) in each energy bin by subtracting the partial current density in downward direction (toward the ionosphere) from the upward direction (from the ionosphere) in both hemispheres. We summed the partial currents to obtain the currents of each electron population (e.g thermal/cold 1–10 eV, warm 10–400 eV, suprathermal/hot 400 eV–26 keV).

[10] The moments (density N_e and parallel $T_{\|}$ and perpendicular $T_{\perp}$ temperatures) of the electron populations were calculated using the integration method on the measured distribution function. Before the calculation of the moments, we took care by applying the spacecraft potential (negative and positive) correction to the distribution function *Lewis et al.* [2008, 2010].

3. Results

[11] Figure 1 shows the average energy-distance electron spectrograms (per pitch angle direction and hemisphere) in differential energy flux (DEF) in $m^{-2}\ s^{-1}\ sr^{-1}$ near Saturn's equatorial rotational plane between 3 and 20 R_S. The figure is composed of 8 panels. The left column panels (a, b, c, d) show from the top to the bottom the electron spectrogram in the downward (180° pitch angle), perpendicular (90° pitch angle), and upward direction (0° pitch angle), and the statistical coverage (number of samples in each direction) in the Northern hemisphere. The right column panels (e, f, g, h) display the same information for the Southern hemisphere. In these spectrograms we observe the three main electron populations present in Saturn's inner magnetosphere: the thermal (i.e. cold, 1–10 eV), warm (10–400 eV) and suprathermal (i.e. hot, 400 eV–26 keV) electron populations. The thermal and suprathermal were first identified in Voyager era by *Sittler et al.* [1983] and then confirmed by the first Cassini results [*Young et al.*, 2005]. Their characteristics and origin were analyzed and discussed by *Rymer et al.* [2008] and *Schippers et al.* [2008]. The thermal and suprathermal electron populations originate respectively from the inner and outer magnetosphere (inside and outside 20 R_S respectively). Both populations were observed to display a pancake-like angular distribution in the innermost magnetosphere and evolve to more field-aligned angular distributions outside of 9–10 R_S [*Schippers et al.*, 2008; *Carbary et al.*, 2011]. The 'warm' electron population was previously identified by *DeJong et al.* [2010] as being

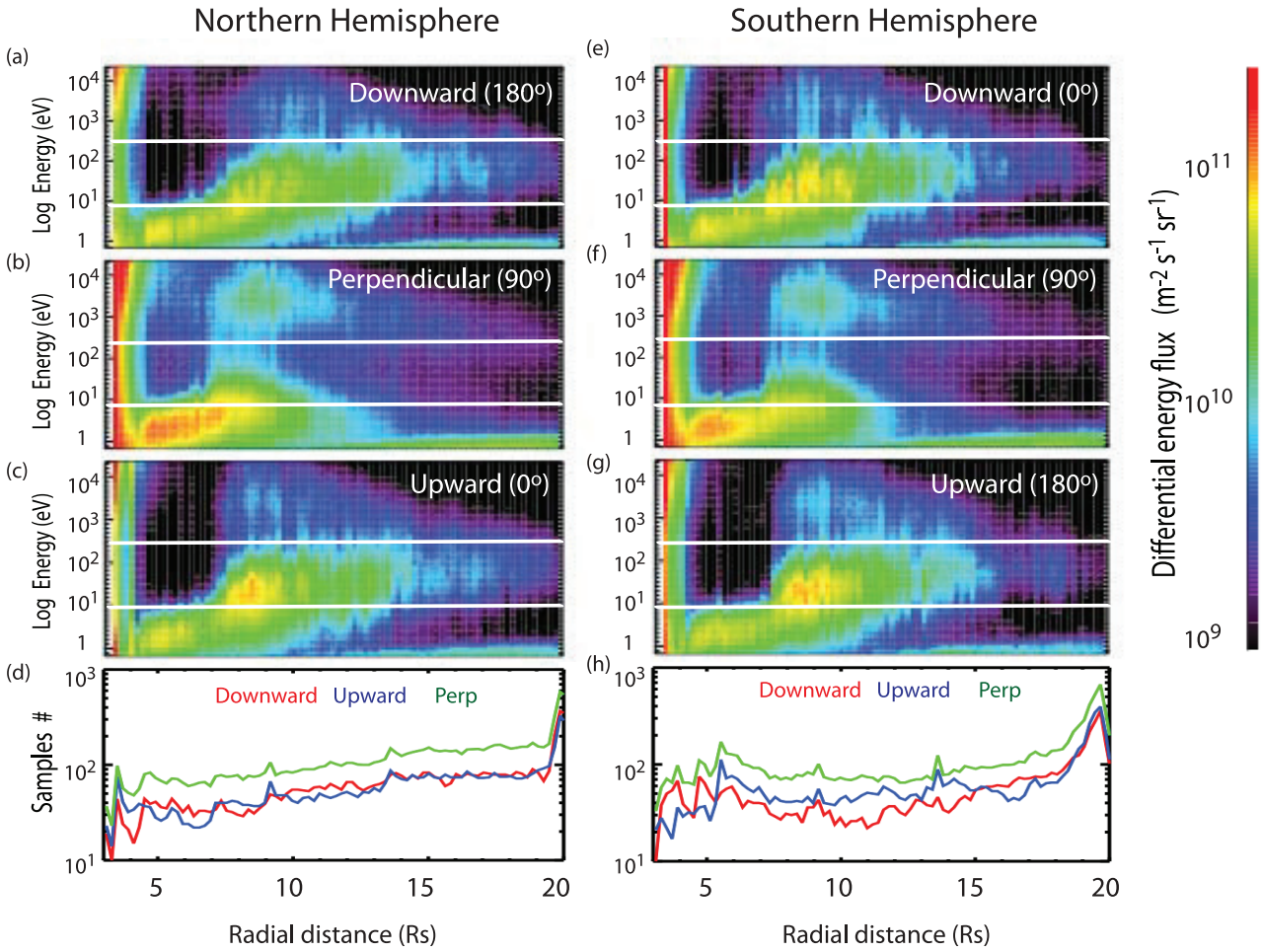

Figure 1. Electron Differential Energy Flux Spectrogram as a function of the radial distance in the (left) Northern and (right) Southern hemisphere, in the (a, e) downward, (b, f) perpendicular and (c, g) upward directions. (d, h) The statistical coverage (number of samples) for the 15 min averaged data in each pitch angle sector in 0.2 R_S wide radial distance bins.

related to interchange events and is characterized by a field-aligned angular distribution.

[12] The density N_e and temperature T_e of the three electron populations derived from the average electron energy spectrogram are presented in Figures 2a and 2b. Because the temperatures of the electron populations are very different, the temperature of the cold population has been multiplied by 5 and the temperature of the hot temperature has been divided by 5 to highlight the profile trend in Figure 2b. We observe that the thermal electron population dominates the density in the inner magnetosphere, then becomes negligible in the outer magnetosphere. Its temperature is low (2 eV) and doesn't vary significantly as a function of the radial distance. The suprathermal electron density is low in the inner magnetosphere, increases up to 9 R_S, then decreases outwards. Its temperature is high (1000 eV) and roughly follows the same trend as the density, similar to the suprathermal moment profiles determined in the case study presented in *Schippers et al.* [2008]. The warm electron population density appears to be low in the innermost magnetosphere and displays the same radial profile trend as the suprathermal electron density. Its temperature is however observed to increase continuously outwards, which is opposite to the trend of the thermal and suprathermal electron population temperatures.

[13] Figure 2c displays an estimation of the maximum current density electrons can carry without field-aligned acceleration, expressed in terms of the density N_e and the temperature T_e ($j_{\|} = eN_e\left(\frac{T_e}{2\pi m_e}\right)^{1/2}$, where m_e is the mass of the electron and e is the electric charge). We observe that the thermal electron population contribution to the current dominates inside 9 R_S while the warm and the hot electron contributions dominate beyond 9 R_S.

[14] Figure 3 displays, for the 'symmetric' case (i.e. no local time separation), the energy-distance spectrograms of the net upward current density (i.e. downward electron flow, left panels) and the net downward current density (i.e. upward electron flow, right panels) in the Northern and Southern hemispheres (top and bottom panels respectively). First, we observe that the current density carried by the cold electrons (below 10 eV) is globally directed upward (i.e.

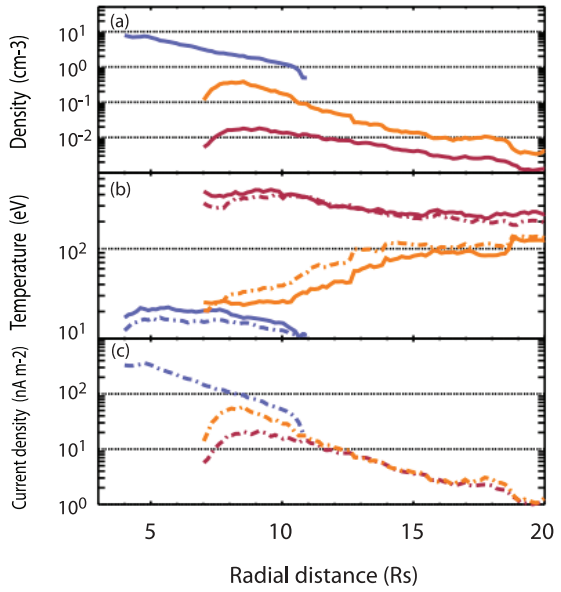

Figure 2. (a) Density, (b) Temperature and (c) Current density of the cold/thermal (×5, blue), warm (orange) and hot/suprathermal (×0.2, red) electron populations as a function of radial distance near the plasma sheet. In Figure 2b, the dashed lines indicate the parallel direction while the solid lines indicate the perpendicular direction. We took care to apply the spacecraft potential (negative and positive) correction before calculating the electron moments.

downward electron flow) in both hemispheres up to 7–8 R_S. Between 8–10 R_S, the current carried by the warm electron population is dominant and directed downward. At 8 R_S, we note the presence of a small-scale signature of inter-hemispheric current directed upward in the Southern hemisphere and downward in the Northern hemisphere. Beyond 10 R_S, no obvious trend for the electric current direction is observed. In this symmetric view, the electric current system in Saturn's inner magnetosphere seems to be structured in two successive layers of upward current inside 8 R_S (region A), downward current between 8 R_S and 10 R_S (region B), and an embedded layer of inter-hemispheric current. Beyond 10 R_S (region C), we don't report any evidence for a specific trend. We note that the region A co-locates the region 1 identified by *Schippers et al.* [2008], which is mainly dominated by the thermal electrons. We also note that the region B is co-located with the boundary (or transition) region between regions 1 and 2, where the plasma is no longer dominated by the thermal electrons but by the effect of a warm/hot electron population which increases the electron plasma pressure (and the plasma beta) in the outer magnetosphere [*Schippers et al.*, 2008].

[15] Figures 4a and 5a display the energy-distance spectrograms of the net upward and downward currents as in Figure 3 for the dayside and the nightside local times respectively. Figures 4b and 5b show the currents of each electron population, after selecting the most reliable data (the ratio of the error on the absolute value must be lower than 1). Positive (negative) current values signify upward (downward) directed currents.

[16] Concerning the dayside results, Figures 4a and 4b show first that, in region A and inside 5 R_S, there is a North-South

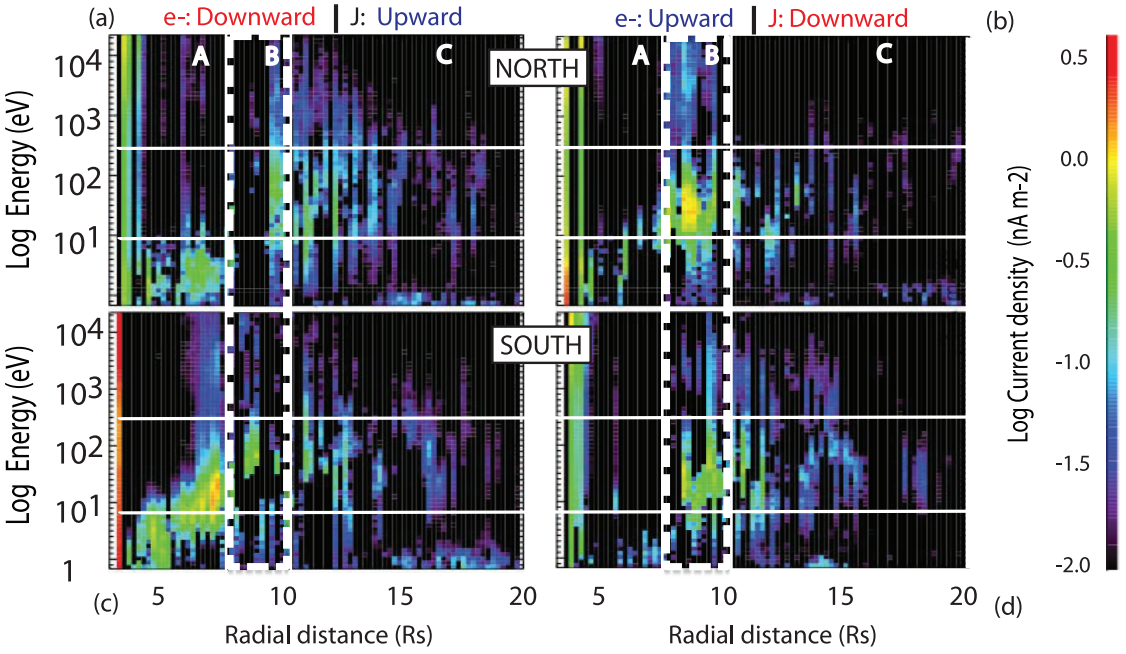

Figure 3. Net Current density per Energy as a function of the radial distance to Saturn in the (top) Northern and (bottom) Southern hemispheres. (a, c) Upward current (downward electron flow) and (b, d) downward current (upward current flow). The white dotted vertical lines identify the different regions. The horizontal white lines separate the thermal (1–10 eV), warm (10–400 eV), and suprathermal (400 eV–26 keV) electron populations.

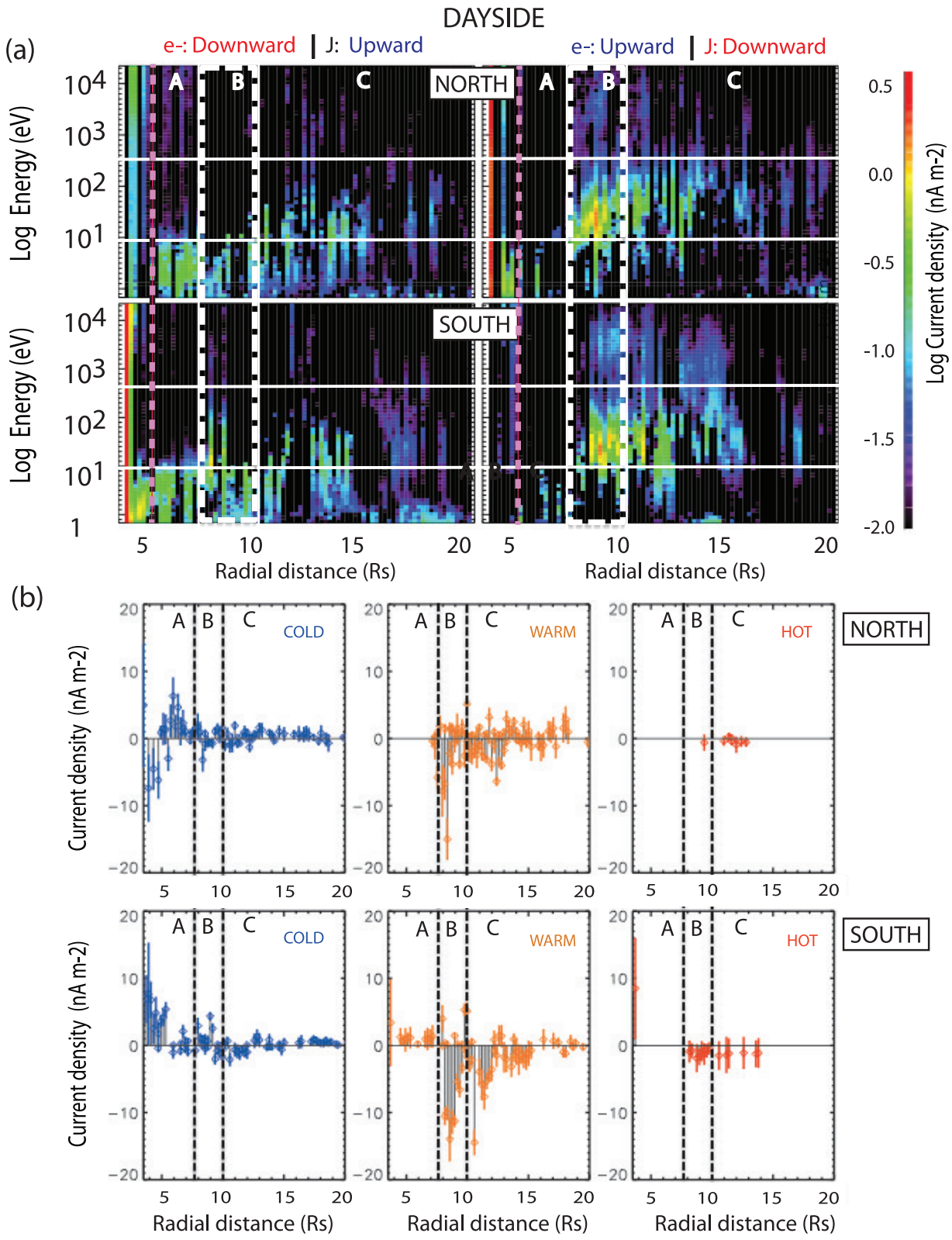

Figure 4. (a) Same as in Figure 3 in the dayside. (b) Current density of the electron populations (cold, warm and hot) in the (top) Northern and (bottom) Southern hemispheres in a stick plot, with error bars (relative error < 1). Positive FAC intensity represents an upward current, and negative FAC intensity represents a downward current.

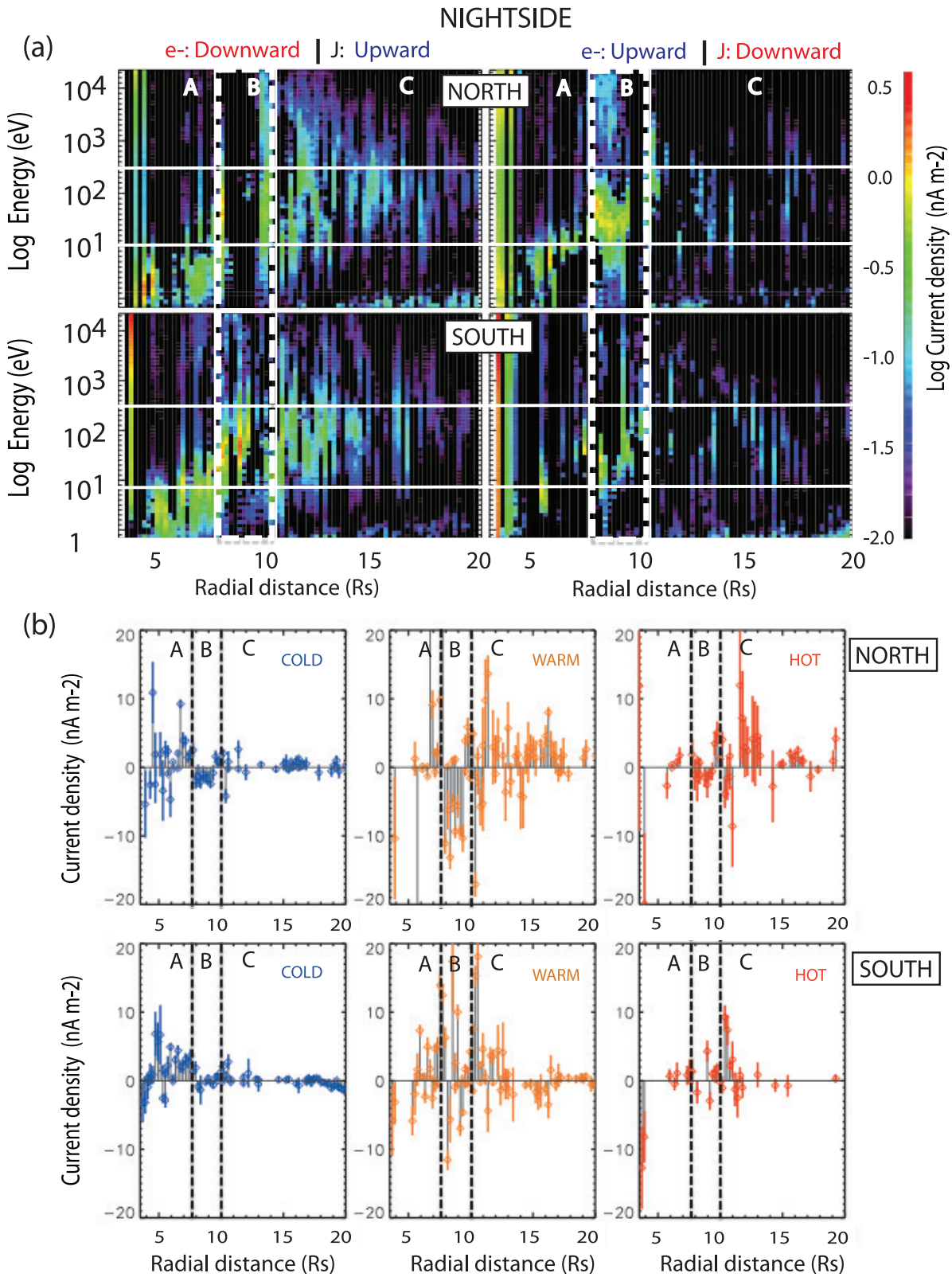

Figure 5. Same as in Figure 4 based on local time in the nightside.

asymmetry of the current carried by the cold electrons, which is directed downward (i.e. upward electron flow) in the Northern hemisphere and directed upward (i.e. downward electron flow) in the Southern hemisphere. If those currents are coupled, then they constitute an inter-hemispheric current directed from the Southern to the Northern hemisphere. Outside of 5 R_S, the current carried by the cold electrons is essentially directed upward (downward electron flow) in both

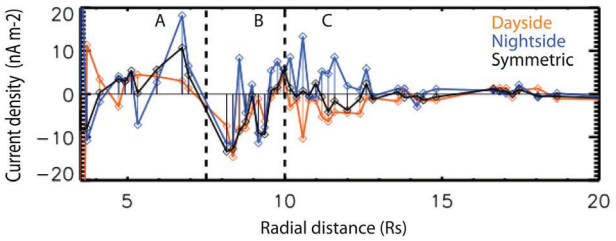

Figure 6. Radial profile of the total current density (summed on all the electron populations) in the dayside, nightside and in the symmetric case (no local time parsing of the dataset).

hemispheres, similar to the symmetric case, and even observed further out but with reduced intensity. In region B, the current density, essentially carried by the warm electrons, appears to be directed downward (i.e. upward electron flow) with similar intensities in the Northern and the Southern hemispheres. This layer of upward current is observed to extend into region C, beyond 10 R_S. Between 13 and 16 R_S, we observe a change in the character of the warm electron current (Figure 4b, middle column), which appears to be oppositely directed in the two hemispheres, respectively upgoing in the North and downgoing in the South, typical of an inter-hemispheric current signature. We observe that the hot electrons are mainly carrying a net downward current in a layer extending from region B to region C.

[17] Concerning the nightside results, Figures 5a and 5b show that, in region A and inside 5 R_S, a succession of layers of downward, upward and inter-hemispheric currents is observed in both hemispheres. At 5–8 R_S, the current carried by the cold electrons is directed upward (i.e. downward electron flow) as in the symmetric case and in the dayside. In region B, the current carried by the warm electrons is essentially directed downward (i.e. upward electron flow) in the Northern hemisphere while a current layer fluctuating between downward and upward is observed in the Southern hemisphere. This is consistent with the presence of embedded layers of downward currents and inter-hemispheric currents directed from the southern to the northern hemisphere. In region C and up to 14 R_S, the current carried by the warm electrons seems to be globally directed upward (i.e. downward electron flow) in both hemispheres while signatures of small-scale inter-hemispheric currents are observed. Outside of 14 R_S, there seems to be a layer of inter-hemispheric currents carried by the warm electron population, directed upward in the Northern hemisphere and downward in the Southern hemisphere, as observed in the dayside. We note that the current carried by the hot electrons is globally directed upward in region C, which is opposite to the observed hot electron current direction in the dayside.

[18] Figure 6 shows the total current density summed on all electron population contributions for the dayside, nightside and in the symmetric case (no local time parsing.) This global picture confirms the previous analysis. Indeed, in region A, all currents appear mainly upward, turning into downward currents inside region B (with an embedded upward component in the nightside). In region C, the currents in the nightside and dayside appear to be oppositely directed (respectively upward and downward), consistent with the symmetric current approaching zero in this region. Finally, the strength of the currents finally seems to weaken at larger radial distance.

4. Discussion and Conclusion

[19] According to our results, the observed current system results from the superposition of (1) layers of 'symmetric' upward current carried by cold electrons in region A and downward current carried by warm electrons in region B, (2) layers of inter-hemispheric current in the nightside and dayside flowing mainly from the Southern to the Northern hemisphere in region A (carried by cold electrons) and in the opposite direction in region C (carried by warm electrons), and (3) layers of local time asymmetric current carried by the warm and hot electrons, flowing in opposite directions in the dayside and nightside.

[20] As discussed in the introduction, sub-corotation occurs in Saturn's inner magnetosphere very close to the planet [*Wilson et al.*, 2009]. *Cowley and Bunce* [2003] described and derived a simple theoretical expression of the expected (1) ionospheric Pedersen currents

$$I_{hP} = \Sigma_P \Omega_S B_{ip} R_i(\theta) \sin(\theta) \left(1 - \frac{\omega}{\Omega_S}\right) \left(\frac{B_i}{B_{ip}}\right) \quad (1)$$

(where Σ_P is the effective height-integrated ionospheric Pedersen conductivity, Ω_S the angular velocity of the planet, B_i the magnetic field strength in the ionosphere, B_{ip} the dipole term of B_i at the poles, R_i the radial distance of the conducting layer of the ionosphere, θ the co-latitude, and ω the angular velocity of magnetospheric shells) and (2) the field-aligned currents FACs

$$j_{\|i}(\theta) = -\frac{n_r}{2\pi R_i^2(\theta)\sin(\theta)} \frac{Bi}{B_{in}} \frac{dI_{hP}}{d\theta} \quad (2)$$

(where n_r is the radial component of the normal to the conducting layer and B_{in} the component of the ionospheric magnetic field normal to the surface) associated with the enforcement of the corotation. We used the azimuthal velocity determined by *Wilson et al.* [2008] on the basis of a statistical study inside 5–10 R_S to derive an estimation of the FAC using the model of *Cowley and Bunce* [2003]. The azimuthal velocity normalized to the corotation speed is presented in the top panel of Figure 7. The ionospheric Pedersen current (I_{hP}) and the FAC (proportional to the derivative of I_{hP}) are presented in the middle panel and bottom panels of the same figure (thick black line). Positive FAC intensity represents an upward current and negative FAC represents a downward current. We observe that the predicted FAC model is composed of a layer of upward currents at radial distances between 5 and 7 R_S which roughly corresponds to our region A, followed by a layer of downward currents beyond 7 R_S corresponding to our region B. The FAC model is presented together with the total electron current density we derived from the electron measurements of CAPS/ELS (represented by diamond symbols). The comparison between the model and the measured currents shows that the observed currents are consistent with the current system enforcing the corotation in Saturn's inner magnetosphere. We previously noted that in region A, the current is mainly carried by the (downgoing) cold electrons,

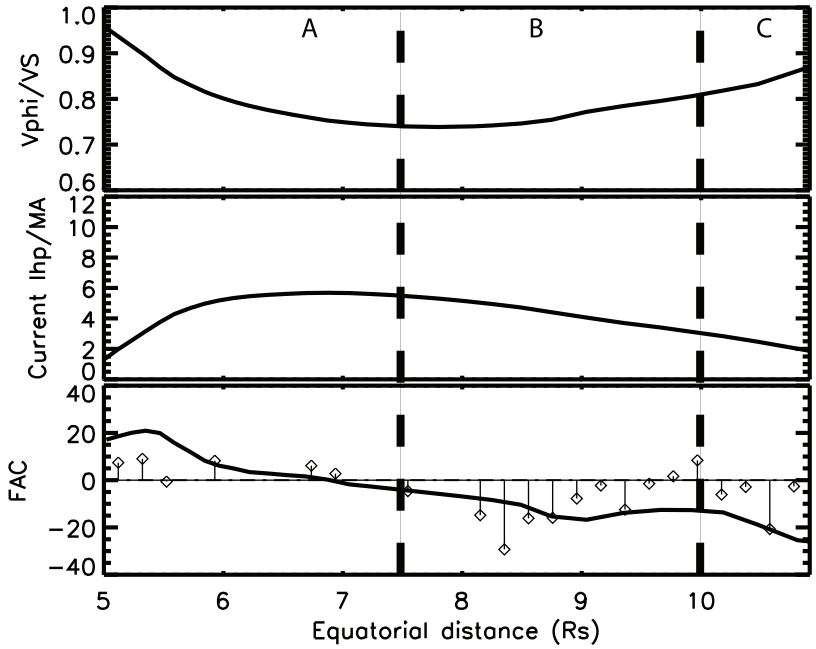

Figure 7. (top) Azimuthal plasma velocity normalized to the corotation velocity, derived from a statistical study on the ion population moments [*Wilson et al.*, 2008]. (middle and bottom) Ionospheric Pedersen current and field-aligned current(FAC) calculated according to the theoretical expressions described in *Cowley and Bunce* [2003]. Positive FAC intensity represents an upward current and negative FAC represents a downward current. The diamonds represent the total current density determined in the dayside, considering both the Northern and the Southern hemispheres.

while in region B the current is carried by the (upgoing) warm electrons. The difference in energy of the two current carrying populations is likely due to the lack of current carriers (low electron density) at high latitude which requires an acceleration of the upgoing electrons to carry the required downward current in region B.

[21] At Earth, inter-hemispheric currents are thought to be triggered by different ionospheric conductances in the Northern and Southern hemispheres due to the asymmetric solar illumination of the hemispheres (e.g. near solstice) or by differences in the source of ionospheric currents (related to the dynamo effect of thermospheric winds or the effects of the interplanetary magnetic field) as reported by *Richmond and Roble* [1987] and *Benkevich et al.* [2000]. If the currents are driven by different ionospheric conductances, we would expect to see a minimum in the inter-hemispheric currents at the Equinox. We note that this point is not demonstrated in our present analysis but seasonal effects will be analyzed in a later study. Since the beginning of the Cassini mission, Saturn's Southern hemisphere has been receiving more solar radiation flux with a possible enhancement of the conductivity in this hemisphere. The inter-hemispheric currents we observe are mainly directed from the North to the South in the innermost magnetosphere, while the apparent closing currents seem to flow from South to North around 13–15 R_S. We note that the presence of inter-hemispheric currents has been recently evoked in studies of *Southwood and Kivelson* [2009] as the source of a rotating dipole in the outer magnetosphere to explain the oscillation of the magnetic field. However, due to the insufficient coverage after the 2009 Saturnian equinox, we did not study the seasonal effects.

[22] The local time asymmetry we identified in the current carried by the warm electrons in regions 2 and 3 complements the list of the previously reported dayside-nightside asymmetries identified in the ring current [*Krimigis et al.*, 2007], the radiation belts [*Paranicas et al.*, 2010], the energetic particle distribution [*Sergis et al.*, 2009], the ENA emission [*Carbary et al.*, 2008], the displacement of the icy satellite micro signatures [*Roussos et al.*, 2007], the ion temperature (M. Thomsen, private communication, 2011), the upper hybrid frequency (fUH) intensity drop near A-ring (2.3 R_S) (D. A. Gurnett, private communication, 2011) and the flux of the low-energy electrons [*DeJong et al.*, 2011]. *Roussos et al.* [2007] and *Paranicas et al.* [2010] reported that the ubiquitous asymmetry could be related to the presence of a weak noon-to-midnight electric field ($\simeq 5 \times 10^{-4} V/m$), probably associated with a dusk-to-dawn plasma flow (M. Thomsen, private communication, 2011). Such an electric field would produce upward currents close to the planet in the dayside and downward current in the nightside. These currents close then in the ionosphere and opposite directed currents appear further out. The current direction in region B and the 'return' currents in region C are consistent with the existence of the noon-to-midnight convective electric field.

[23] The interpretation of our analysis is summarized in the sketch presented in Figures 8a and 8b. Panel a displays the current carriers of the observed currents and panel b shows the combination of the three assumed current systems: (1) a current system derived from corotation-enforcement (in blue), (2) a IHFAC system (in green), and (3) a noon-to-midnight electric field (in red). We note that the magnetic field configuration represented in this sketch is only an

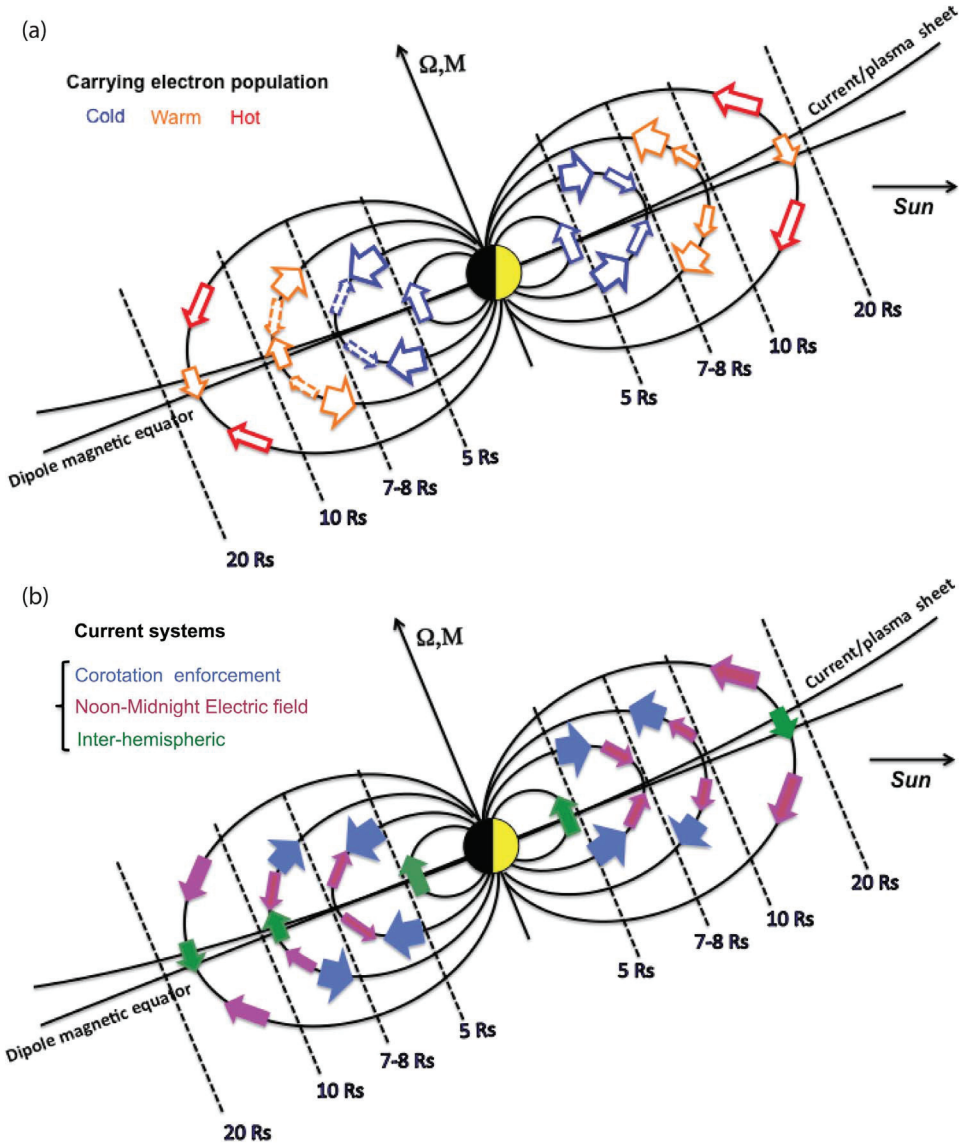

Figure 8. Sketch representing the electric current systems which might be present in Saturn's magnetosphere. The arrows represent the direction of the currents and arrows with dashed contour indicate the currents which are not directly observed but inferred from our analysis. (a) The arrow contour is indicative of the electron population which carries the current. (b) The arrow color filling is indicative of the current system. We note that the magnetic field configuration represented in this sketch is only an approximation and does not attempt to depict accurately the magnetic field lines distortion beyond 12 R_S in the nightside.

approximation and does not attempt to depict accurately the distortion of the field lines in the nightside beyond 12 R_S.

[24] The identification of magnetospheric regions with magnetic field lines carrying net downward electron flow raises the question of the role of these electron flows as a generator of ionospheric signatures such as auroras. Saturn's main auroral oval was found to map to the open/closed field line boundary [*Bunce et al.*, 2008] in the outer magnetospheric region (beyond 20 R_S). By analyzing the energetic electron data of the MIMI instrument (from 20 keV to tens of MeV) during the first Cassini orbits near the equatorial plane, *Saur et al.* [2006] identified bidirectional (both downward and upward) electron beams mapping the location of Saturn's main aurora. A couple of years later, *Mitchell et al.* [2009] identified electron beams and ion conics in the high-latitude downward current sheet regions which present a lot of similarities with the auroral downward current region observed at Earth, located at the proximity of upward current regions mapping the bright aurora. A recent study from *Grodent et al.* [2010] revealed the presence of an outer UV auroral emission at Saturn, equatorward of the main auroral oval in Saturn's southern polar region. This newly identified UV emission was found to map to a region in the equatorial plane between 4 and 11 R_S and was only observed in the nightside. The authors estimated that the keV electrons constituting the suprathermal electron population [*Schippers et al.*, 2008] at the equator have sufficient energy to generate the observed outer UV auroral emission.

In our analysis, we identified a strong day-night asymmetry of the hot electron flow direction in regions 2–3, mainly directed upward in the dayside while observed to be directed downward in the nightside precisely where the outer UV aurora is observed. A secondary infrared auroral oval was also identified equatorward of the main auroral oval by *Stallard et al.* [2008, 2010] and is believed to be associated with corotation breakdown in the magnetospheric plasma as is the case for the generation of main auroral UV at Jupiter. *Stallard et al.* [2010] mapped the location of the auroral feature to the magnetosphere, at a distance as close as Enceladus' orbit (3.9 R_S) and beyond. According to the authors, the absence of significant UV counterpart at those latitudes means that the emissions may be induced by the precipitation of electrons with low energies, sufficient to excite the IR aurora but not the UV. As an example, the energies necessary to generate the brightness of the outer auroral oval must range from 0.2 to 3 keV according to *Grodent et al.* [2010]. In our analysis, we identified a layer of net downward-directed thermal electrons with very low energy in region A which may be a suitable candidate to generate the secondary IR aurora.

[25] In conclusion, we have identified, from the analysis of an extended electron dataset, the presence of layers of net upward and downward current whose origin is consistent with the superposition of large-scale current systems induced by the corotation enforcement, the presence of a local time dependent electric field and differential conductivities between the northern and southern hemispheres. Further coverage will permit the study of the longitudinal dependence of the current systems identified in Saturn's magnetosphere.

[26] **Acknowledgments.** The research at the University of Iowa was supported by the National Aeronautics and Space Administration through contract 1356500 with the Jet Propulsion Laboratory. Cassini CAPS Data analysis at IRAP was supported by CNES. A.J.C. and G.R.L. were supported by STFC funding to MSSL/UCL.

[27] Masaki Fujimoto thanks the reviewers for their assistance in evaluating this paper.

References

Arridge, C. S., K. K. Khurana, C. T. Russell, D. J. Southwood, N. Achilleos, M. K. Dougherty, A. J. Coates, and H. K. Leinweber (2008), Warping of Saturn's magnetospheric and magnetotail current sheets, *J. Geophys. Res.*, *113*, A08217, doi:10.1029/2007JA012963.

Badman, S. V., S. W. H. Cowley, J.-C. Gérard, and D. Grodent (2006), A statistical analysis of the location and width of Saturn's southern auroras, *Ann. Geophys.*, *24*, 3533–3545, doi:10.5194/angeo-24-3533-2006.

Benkevich, L., W. Lyatsky, and L. L. Cogger (2000), Field-aligned currents between conjugate hemispheres, *J. Geophys. Res.*, *105*, 27,727–27,738, doi:10.1029/2000JA900095.

Bunce, E. J., et al. (2008), Origin of Saturn's aurora: Simultaneous observations by cassini and the Hubble space telescope, *J. Geophys. Res.*, *113*, A09209, doi:10.1029/2008JA013257.

Carbary, J. F., D. G. Mitchell, C. Paranicas, E. C. Roelof, and S. M. Krimigis (2008), Direct observation of warping in the plasma sheet of Saturn, *Geophys. Res. Lett.*, *35*, L24201, doi:10.1029/2008GL035970.

Carbary, J. F., D. G. Mitchell, C. Paranicas, E. C. Roelof, S. M. Krimigis, N. Krupp, K. Khurana, and M. Dougherty (2011), Pitch angle distributions of energetic electrons at Saturn, *J. Geophys. Res.*, *116*, A01216, doi:10.1029/2010JA015987.

Cowley, S. W. H., and E. J. Bunce (2003), Corotation-driven magnetosphere-ionosphere coupling currents in Saturn's magnetosphere and their relation to the auroras, *Ann. Geophys.*, *21*, 1691–1707, doi:10.5194/angeo-21-1691-2003.

DeJong, A. D., J. L. Burch, J. Goldstein, A. J. Coates, and D. T. Young (2010), Low-energy electrons in Saturn's inner magnetosphere and their role in interchange injections, *J. Geophys. Res.*, *115*, A10229, doi:10.1029/2010JA015510.

DeJong, A. D., J. L. Burch, J. Goldstein, A. J. Coates, and F. Crary (2011), Day-night asymmetries of low-energy electrons in Saturn's inner magnetosphere, *Geophys. Res. Lett.*, *38*, L08106, doi:10.1029/2011GL047308.

Espinosa, S. A., and M. K. Dougherty (2001), Unexpected periodic perturbations in Saturn's magnetic field data from Pioneer 11 and Voyager 2, *Adv. Space Res.*, *28*, 919–924, doi:10.1016/S0273-1177(01)00518-X.

Grodent, D., A. Radioti, B. Bonfond, and J.-C. Gérard (2010), On the origin of Saturn's outer auroral emission, *J. Geophys. Res.*, *115*, A08219, doi:10.1029/2009JA014901.

Gurnett, D. A., J. B. Groene, A. M. Persoon, J. D. Menietti, S.-Y. Ye, W. S. Kurth, R. J. MacDowall, and A. Lecacheux (2010), The reversal of the rotational modulation rates of the north and south components of Saturn kilometric radiation near equinox, *Geophys. Res. Lett.*, *37*, L24101, doi:10.1029/2010GL045796.

Khurana, K. K., D. G. Mitchell, C. S. Arridge, M. K. Dougherty, C. T. Russell, C. Paranicas, N. Krupp, and A. J. Coates (2009), Sources of rotational signals in Saturn's magnetosphere, *J. Geophys. Res.*, *114*, A02211, doi:10.1029/2008JA013312.

Krimigis, S. M., N. Sergis, D. G. Mitchell, D. C. Hamilton, and N. Krupp (2007), A dynamic, rotating ring current around Saturn, *Nature*, *450*, 1050–1053, doi:10.1038/nature06425.

Lewis, G. R., N. André, C. S. Arridge, A. J. Coates, L. K. Gilbert, D. R. Linder, and A. M. Rymer (2008), Derivation of density and temperature from the Cassini-Huygens CAPS electron spectrometer, *Planetary Space Sci.*, *56*, 901–912, doi:10.1016/j.pss.2007.12.017.

Lewis, G. R., et al. (2010), The calibration of the Cassini-Huygens CAPS electron spectrometer, *Planetary Space Sci.*, *58*, 427–436, doi:10.1016/j.pss.2009.11.008.

Mitchell, D. G., et al. (2009), Ion conics and electron beams associated with auroral processes on Saturn, *J. Geophys. Res.*, *114*, A02212, doi:10.1029/2008JA013621.

Paranicas, C., et al. (2010), Asymmetries in Saturn's radiation belts, *J. Geophys. Res.*, *115*, A07216, doi:10.1029/2009JA014971.

Richardson, J. D. (1998), Thermal plasma and neutral gas in Saturn's magnetosphere, *Rev. Geophys.*, *36*, 501–524, doi:10.1029/98RG01691.

Richmond, A. D., and R. G. Roble (1987), Electrodynamic effects of thermospheric winds from the NCAR thermospheric general circulation model, *J. Geophys. Res.*, *92*, 12,365–12,376, doi:10.1029/JA092iA11p12365.

Roussos, E., et al. (2007), Electron microdiffusion in the Saturnian radiation belts: Cassini MIMI/LEMMS observations of energetic electron absorption by the icy moons, *J. Geophys. Res.*, *112*, A06214, doi:10.1029/2006JA012027.

Rymer, A. M., B. H. Mauk, T. W. Hill, C. Paranicas, D. G. Mitchell, A. J. Coates, and D. T. Young (2008), Electron circulation in Saturn's magnetosphere, *J. Geophys. Res.*, *113*, A01201, doi:10.1029/2007JA012589.

Saur, J., B. H. Mauk, A. Kaßner, and F. M. Neubauer (2004), A model for the azimuthal plasma velocity in Saturn's magnetosphere, *J. Geophys. Res.*, *109*, A05217, doi:10.1029/2003JA010207.

Saur, J., et al. (2006), Anti-planetward auroral electron beams at Saturn, *Nature*, *439*, 699–702, doi:10.1038/nature04401.

Schippers, P., et al. (2008), Multi-instrument analysis of electron populations in Saturn's magnetosphere, *J. Geophys. Res.*, *113*, A07208, doi:10.1029/2008JA013098.

Sergis, N., S. M. Krimigis, D. G. Mitchell, D. C. Hamilton, N. Krupp, B. H. Mauk, E. C. Roelof, and M. K. Dougherty (2009), Energetic particle pressure in Saturn's magnetosphere measured with the magnetospheric imaging instrument on Cassini, *J. Geophys. Res.*, *114*, A02214, doi:10.1029/2008JA013774.

Sittler, E. C., Jr., K. W. Ogilvie, and J. D. Scudder (1983), Survey of low-energy plasma electrons in Saturn's magnetosphere: Voyagers 1 and 2, *J. Geophys. Res.*, *88*, 8847–8870, doi:10.1029/JA088iA11p08847.

Southwood, D. J., and M. G. Kivelson (2007), Saturnian magnetospheric dynamics: Elucidation of a camshaft model, *J. Geophys. Res.*, *112*, A12222, doi:10.1029/2007JA012254.

Southwood, D. J., and M. G. Kivelson (2009), The source of Saturn's periodic radio emission, *J. Geophys. Res.*, *114*, A09201, doi:10.1029/2008JA013800.

Stallard, T., S. Miller, H. Melin, M. Lystrup, S. W. H. Cowley, E. J. Bunce, N. Achilleos, and M. Dougherty (2008), Jovian-like aurorae on Saturn, *Nature*, *453*, 1083–1085, doi:10.1038/nature07077.

Stallard, T., H. Melin, S. W. H. Cowley, S. Miller, and M. B. Lystrup (2010), Location and magnetospheric mapping of Saturn's mid-latitude infrared auroral oval, *Astrophys. J.*, *722*, L85–L89, doi:10.1088/2041-8205/722/1/L85.

Talboys, D. L., C. S. Arridge, E. J. Bunce, A. J. Coates, S. W. H. Cowley, and M. K. Dougherty (2009a), Characterization of auroral current

systems in Saturn's magnetosphere: High-latitude Cassini observations, *J. Geophys. Res.*, *114*, A06220, doi:10.1029/2008JA013846.

Talboys, D. L., C. S. Arridge, E. J. Bunce, A. J. Coates, S. W. H. Cowley, M. K. Dougherty, and K. K. Khurana (2009b), Signatures of field-aligned currents in Saturn's nightside magnetosphere, *Geophys. Res. Lett.*, *36*, L19107, doi:10.1029/2009GL039867.

Thomsen, M. F., D. B. Reisenfeld, D. M. Delapp, R. L. Tokar, D. T. Young, F. J. Crary, E. C. Sittler, M. A. McGraw, and J. D. Williams (2010), Survey of ion plasma parameters in Saturn's magnetosphere, *J. Geophys. Res.*, *115*, A10220, doi:10.1029/2010JA015267.

Wilson, R. J., R. L. Tokar, M. G. Henderson, T. W. Hill, M. F. Thomsen, and D. H. Pontius (2008), Cassini plasma spectrometer thermal ion measurements in Saturn's inner magnetosphere, *J. Geophys. Res.*, *113*, A12218, doi:10.1029/2008JA013486.

Wilson, R. J., R. L. Tokar, and M. G. Henderson (2009), Thermal ion flow in Saturn's inner magnetosphere measured by the Cassini plasma spectrometer: A signature of the Enceladus torus?, *Geophys. Res. Lett.*, *36*, L23104, doi:10.1029/2009GL040225.

Young, D. T., et al. (2005), Composition and dynamics of plasma in Saturn's magnetosphere, *Science*, *307*, 1262–1266, doi:10.1126/science.1106151.